Bull. Mater. Sci., Vol. 38, No. 5, September 2015, pp. 1163–1170. © Indian Academy of Sciences.

Synthesis and characterization of silicon-doped polycrystalline GaN films by r.f. sputtering

S GUPTA[1,2]

[1]Department of Materials Science, Indian Association for the Cultivation of Science, Calcutta 700 032, India
[2]Department of Engineering Physics, The Oxford College of Engineering, Bangalore 560 068, India

MS received 22 January 2015; accepted 11 May 2015

Abstract. Silicon-doped polycrystalline GaN films were successfully deposited at temperatures ranging from 300 to 623 K on fused silica and silicon substrates by radio frequency (r.f.) magnetron sputtering at a system pressure of ~ 5 Pa. The films were characterized by optical as well as microstructural measurements. The optical properties were studied by UV–vis–NIR spectrometer and photoluminicence (PL) measurements. The microstructural information was obtained from scanning electron microscope (SEM), energy-dispersive X-ray spectroscopy (EDX), atomic force microscopy (AFM) and X-ray diffraction (XRD) studies. PL measurement at 80 K exhibited two strong transitions located at ~ 2.1 and ~ 2.7 eV along with lower intensity peaks for luminescence at the higher energy side at ~ 3.45 and ~ 3.3 eV for all the films deposited here, and the peaks at ~ 3.45 and ~ 3.3 eV could be ascribed to transitions related to excitons bound to a neutral donor for h-GaN and c-GaN, respectively. A broad peak at ~ 2.1 eV indicated the presence of yellow luminescence in all the films. The SEM and AFM images revealed that the films are compact with well-dispersed polycrystalline constituting the films. The XRD traces contained the signature of both the hexagonal and cubic phases of GaN.

Keywords. Group III nitrides; r.f. sputtering; optical and microstructural properties.

1. Introduction

It is an increasingly accepted fact that the group III nitrides originate from their promising potential for short-wavelength light-emitting diodes, semiconducting lasers and optical detectors, and for high temperature, high power and high frequency devices as well. The main technological interest in the polycrystalline-based devices stems from its very low-cost production. Among different group III nitrides, GaN being a direct bandgap semiconductor has shown great promise towards the above applications.

The control of doping in wide bandgap semiconductors like GaN is difficult due to the formation of native defects. Probability of defect formation increases with the increase in bandgap, while the enthalpy for defect formation is lower than the bandgap energy. Jenkins and Dow[1] concluded from their analysis that the native defects are responsible for the usual n-type character and that a shallow hydrogenic donor in this material can be related to nitrogen vacancy. According to Neugebaur and Van der Walle,[2] nitrogen vacancies seems to be energetically most favourable, followed by antisites and interstitials. At this juncture, what remains to be seen that how Silicon being most common n-type dopant in GaN can rectify the different properties in polycrystalline GaN thin films by radio frequency (r.f.) sputtering.

Depending on the growth conditions, GaN crystallizes either in the stable hexagonal (wurtzite phase) or metastable cubic (zinc blend phase) polytypes. The prevalent deposition techniques for depositing GaN thin films are mainly metal organic chemical vapour deposition (MOCVD) and molecular beam epitaxy (MBE).

It is well documented in the literature that the growth of GaN in polycrystalline form is based on MBE,[3–5] MOCVD[6–8] and post-nitridation technique.[9,10] In recent times, amorphous and polycrystalline GaN thin films have been deposited by using both magnetron sputtering technique[11–14] and laser ablation[15–18] technique. In this communication, the synthesis of polycrystalline silicon (1 at%)-doped GaN films by the r.f. sputtering technique at reasonably lower temperature is reported. The films were characterized by measuring optical and microstructural properties to derive meaningful information in the films.

2. Experimental

Silicon-doped polycrystalline GaN thin films were deposited onto fused silica substrates by r.f. sputtering of a GaN target (99.999%) containing 1 at% Si in argon plasma and a combination of Ar and N_2 plasma at a system

(guptasnigdha646@gmail.com)

pressure of ~5 Pa. The films were deposited at different substrate temperatures ranging from 300 to 623 K and for a fixed deposition time of ~3 h. The substrates were placed on a heavy circular copper block that were heated by appropriate heating coils passing through holes laterally drilled through the copper block. The temperature of the substrates were monitored and controlled by a copper–constantan thermocouple through an on/off electronic temperature controller. Before starting the actual deposition, the target was pre-sputtered with a shutter located in between target and substrate. All the depositions were performed with a 140 W r.f. power from a power supply capable of delivering 1.0 kW, 13.56 mHz. The diameter of the target was 2.5 cm. The distance between the target and substrate was ~3.5 cm. Optical studies were performed by measuring transmittance in the wavelength region of $\lambda = 200$–800 nm using a spectrophotometer (Hitachi-U3410) at room temperature. The spectra were recorded with a resolution of $\lambda \sim 0.07$ nm along with a photometric accuracy of ± 0.3% for transmittance measurements. Scanning electron microscope (SEM) images were obtained from a Hitachi SEM and atomic force microscopy (AFM) images were obtained with Nanoscope-IV (Digital Instruments). Photoluminescence (PL) spectra were recorded using a Perkin Elmer LS55 spectrometer along with a 300 W xenon arc lamp as the emission source. A Hamamatsu photomultiplier was used as the detector along with a 1/4 m monochromator. Fourier transform infrared (FTIR) spectra were recorded by a Nicolet (MAGNA-IR-750) spectrometer.

3. Results and discussion

3.1 *Microstructural study*

The GaN films were deposited by r.f. sputtering onto fused silica substrates kept at different substrate temperatures (T_s), as indicated in table 1. It was observed that films with different grain sizes (D) were obtained by varying the substrate temperatures during sputtering of the GaN target. The SEM images of two representative nanocrystalline GaN films deposited at substrate temperatures at ~423 and 623 K along with the corresponding grain size distribution are shown in figure 1. The SEM images (figure 1a and b) revealed that the films were compact with well dispersed polycrystalline constituting the films. The grain sizes obtained from the SEM pictures varied from 0.18 and 0.35 μm with the increasing substrate temperature during deposition. Gradual increase in grain size was observed for films as the substrate temperature was increased from 300 to 623 K. The grain sizes (D) of the GaN films obtained from optical measurements (discussed later) were found to vary from 0.12 to 0.25 μm (table 1), which tallied well with that obtained from SEM studies. AFM pictures of four representative polycrystalline Si-doped GaN films deposited at 300, 423, 523 and 623 K are shown in figure 2a–d, respectively. One can observe that the grain size increased with the increase in substrate temperature during deposition.

Figure 3 shows the XRD trace of a representative film deposited at 423 K. It may be observed that the XRD data have contained the signature of both the hexagonal and cubic phases of GaN. The spectrum is dominated by sharp and intense peaks corresponding to reflections from (002) plane for c-GaN[3] and another c-GaN peak from (111) plane followed by peaks for h-GaN for reflections from (101), (103), (201), (004) and (202) planes (JCPDS data file). The relative intensity of the peaks for c-GaN and h-GaN decreases for films deposited at lower substrate temperature during deposition. It may also be noted that the peaks became sharper for films deposited at higher substrate temperatures indicating grain growth in these films. The average grain size L can be calculated by Scherer's formula as

$$L = \frac{0.91\lambda}{D\cos\theta},$$

where λ is the wavelength of X-ray and D the full-width at half-maximum (FWHM) of the (0002) reflection peak while θ the Bragg angle. The grain sizes were found to be 0.18, 0.22, 0.24 and 0.32 μm, respectively, which are in agreement with those obtained from optical studies. Furthermore, it was noticed that there was a decrease in the FWHM of (002) peaks with the increase in the film thickness. The latter indicated that the grain size of the poly-GaN, which could be calculated from FWHM of (002) peaks, became larger in thicker films. The result is consistent with that from SEM and AFM. It might be noted here that the films deposited at temperatures between 300 and 423 K showed predominant hexagonal

Table 1. Different parameters obtained from Si-doped polycrystalline GaN deposited at different substrate temperatures.

Film name	Substrate temp. (K)	Thickness (μm)	Roughness (nm)	Grain size (μm)	Bandgap (eV)	N (cm^{-3})
S-1	300	0.20	11	0.12	3.42	9.54×10^{18}
S-2	423	0.22	15	0.16	3.35	9.65×10^{18}
S-3	523	0.27	19	0.21	3.27	9.85×10^{18}
S-4	623	0.30	24	0.25	3.18	2.54×10^{19}

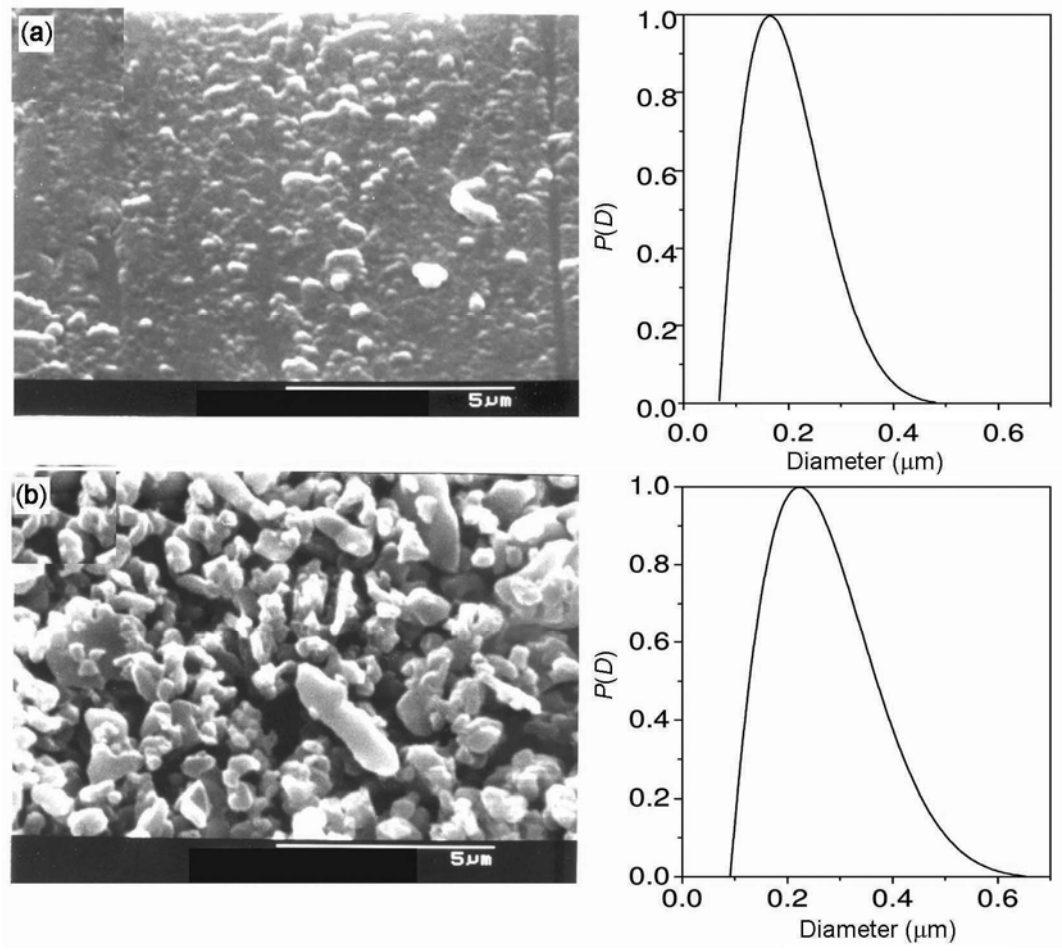

Figure 1. SEM micrographs of two representative Si-doped GaN films deposited at (**a**) 523 and (**b**) 623 K.

phase with reflections from (101) and (103) planes for h-GaN, while those deposited above 523 K indicated predominant cubic phase of GaN showing reflections from (002) and (111) planes of c-GaN. Films deposited at intermediate temperatures were seen to contain mixed phases with a relative content of cubic phase that increased with the increase in T_s. Peaks located at $2\theta =$ 47.5° and 56.2° might be identified with the reflections from (220) and (311) planes of Si. The presence of Si peaks in the XRD pattern may be described as the presence of Si atoms at the surface of the films or it might come from fused silica substrate. The energy-dispersive X-ray spectroscopy (EDX) spectra confirm the presence of Si peaks along with the Ga and N_2 peaks. The elemental detection from EDX measurements reveals 53% N_2, 45% Ga and 2 at% of Si in the presence of Ar + N_2 plasma during the deposition of films and that of 38.5% N_2, 60% Ga and 1.5 at% of Si in the presence of Ar plasma.

3.2 *Bandgap and optical constants*

The absorption coefficients (α) of the Si-doped GaN films were determined by measuring transmittance and reflectance in these films.[19,20] In general, the absorption coefficient (α) may be written as a function of the incident photon energy ($h\nu$) so that

$$\alpha h\nu = B(h\nu - E_g)^m, \tag{1}$$

where m indicates the nature of a particular transition and may be obtained from the plot of $\ln(\alpha h\nu)$ *vs.* $\ln(h\nu - E_g)$, as shown in the inset of figure 4. We estimated $m = 0.48$ for this representative GaN film, which indicated an allowed direct optical transition. The bandgap (E_g) was determined from the plot of $(\alpha h\nu)^2$ *vs.* $h\nu$, as shown in figure 4, for a representative film deposited at $T_s = 300$ K showing $E_g \sim 3.42$ eV. The bandgaps obtained for films deposited at different substrate temperatures (T_s) are shown in figure 5 and table 1. It could be observed that the films deposited at temperatures ~ 300 K had bandgap ~ 3.4 eV, which is equal to the bandgap of h-GaN. Films deposited at subsequently higher temperatures indicated gradual lowering of bandgap attaining ~ 3.2 eV for c-GaN for films deposited at $T_s > 523$ K. This clearly corroborates the observation from the XRD studies that the films deposited at higher temperature ($T > 523$ K)

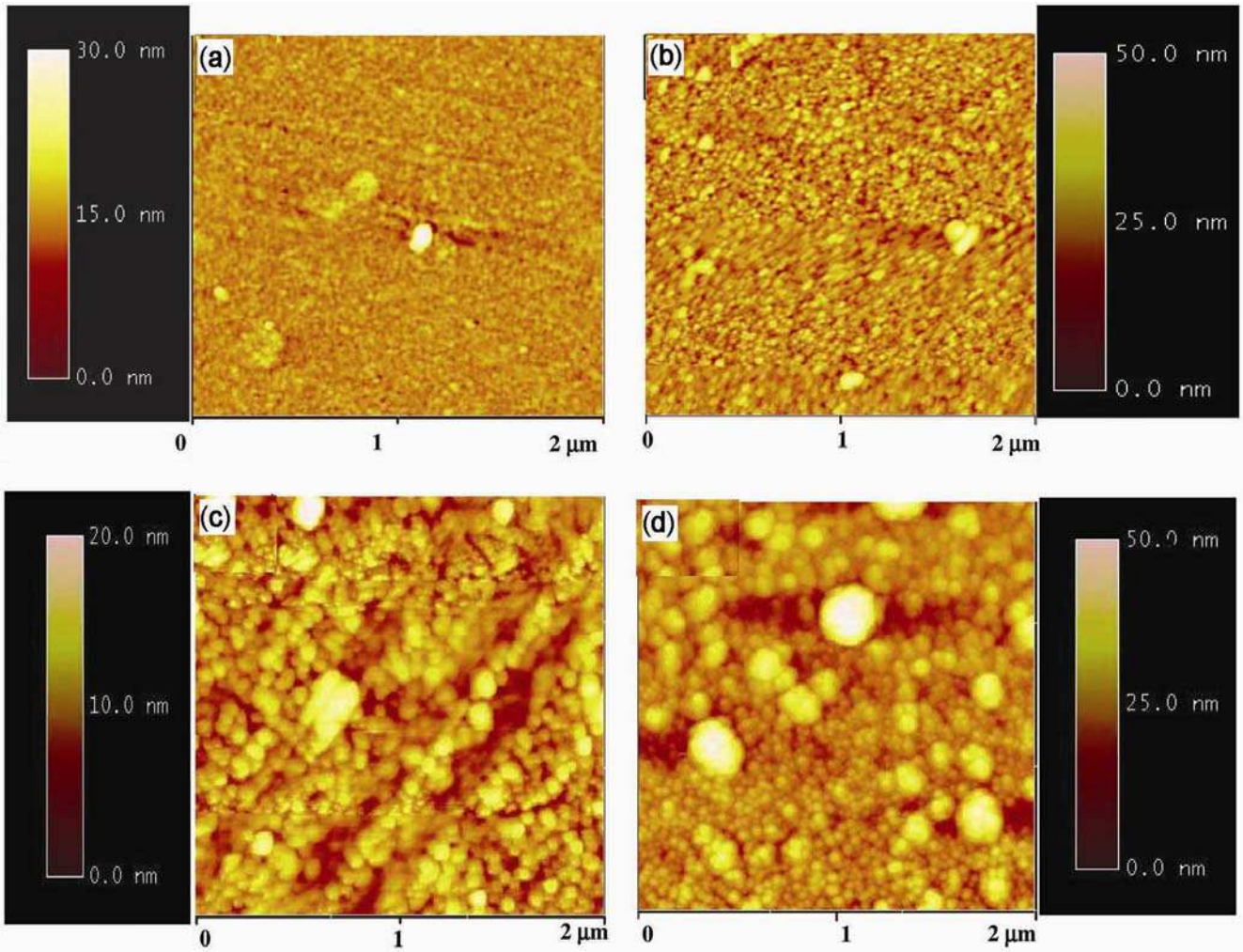

Figure 2. AFM pictures of some representative Si-doped GaN films deposited at (**a**) 300, (**b**) 373, (**c**) 523 and (**d**) 623 K.

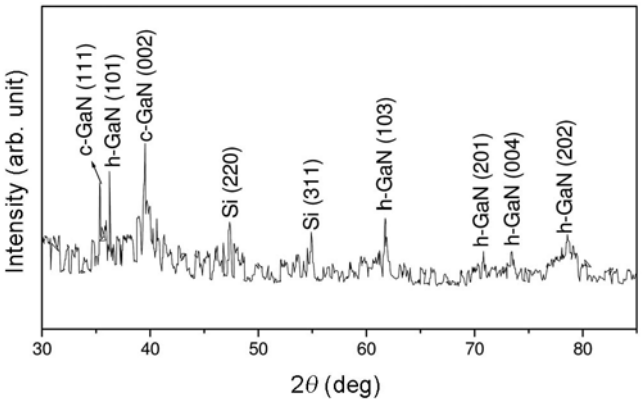

Figure 3. XRD spectrum of a representative film deposited at 623 K.

contained higher c-GaN phase. The optical constants (refractive index n and extinction coefficient k) of the polycrystalline GaN films were determined from the

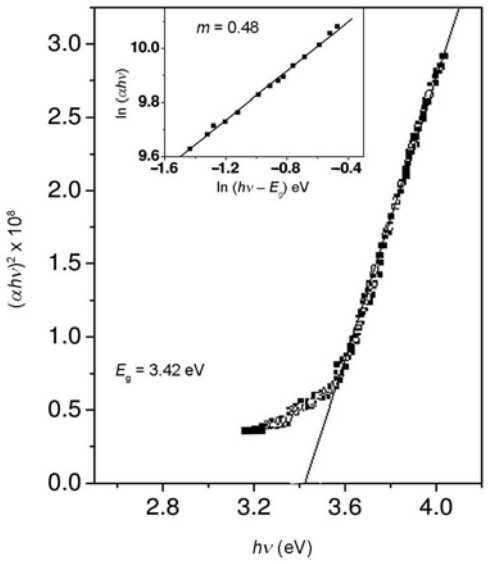

Figure 4. Plot of $(\alpha h\nu)^2$ *vs.* $h\nu$ of a representative film deposited at T_s = 300 K. Inset shows the plot of $\ln(\alpha h\nu)$ *vs.* $\ln(h\nu - E_g)$.

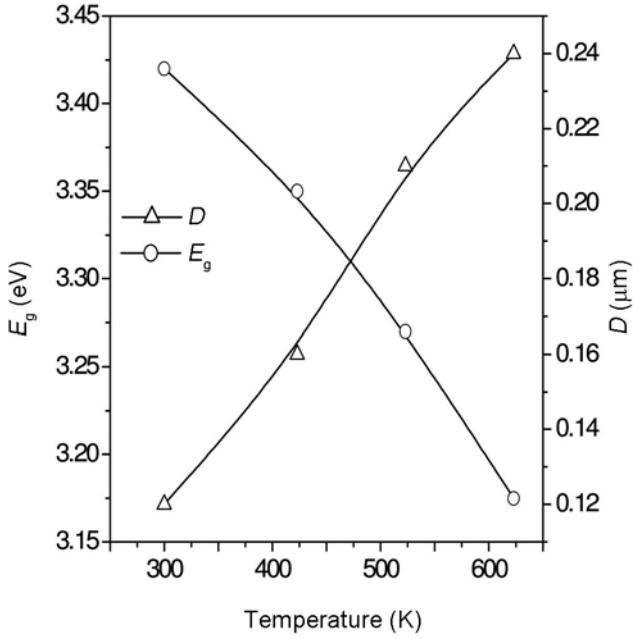

Figure 5. Variation of bandgap (E_g) and grain diameter (D) with substrate temperature (T_s) during deposition.

transmittance and/or reflectance *vs.* wavelength traces by using the standard relations.[19,20] Variation of refractive index and extinction coefficient with $h\nu$ have been shown in figure 6a and b, respectively. It may be observed that the refractive index increased for films deposited at increased substrate temperature during deposition. The refractive index tends to attain the bulk value (~2.1) for c-GaN for films deposited at higher substrate temperature while the absorption coefficient increased significantly for films with higher c-GaN content.

3.3 *Grain distribution and surface roughness*

Surface roughness (σ_0) which is the rms height fluctuations of the surface irregularities can be obtained by recording the diffused part of the reflectance (R_{diff}) from the film surface.[21] We recorded both the specular (R) and diffused (R_{diff}) part of the reflectance and σ_0 was determined from the variation of $R/(R + R_{diff})$ with wavelength (λ) by using the relation[21]

$$\ln[R/R_0] = -(4\pi\sigma_0)^2/\lambda^2 + \text{constant}, \quad (2)$$

where $R_0 = R + R_{diff}$. The surface roughness (σ_0) for the GaN films deposited at different temperatures was obtained from the slopes of the plots (not shown here) of $\ln(R_0/R)$ *vs.* $1/\lambda^2$. The surface roughness (σ_0) varied between 11 and 24 nm (table 1) and the roughness increased for films deposited at higher temperature.

Distribution of grain sizes in these polycrystalline films could also be conveniently evaluated by measuring diffuse (R_{diff}) and specular (R_0) reflections from the film

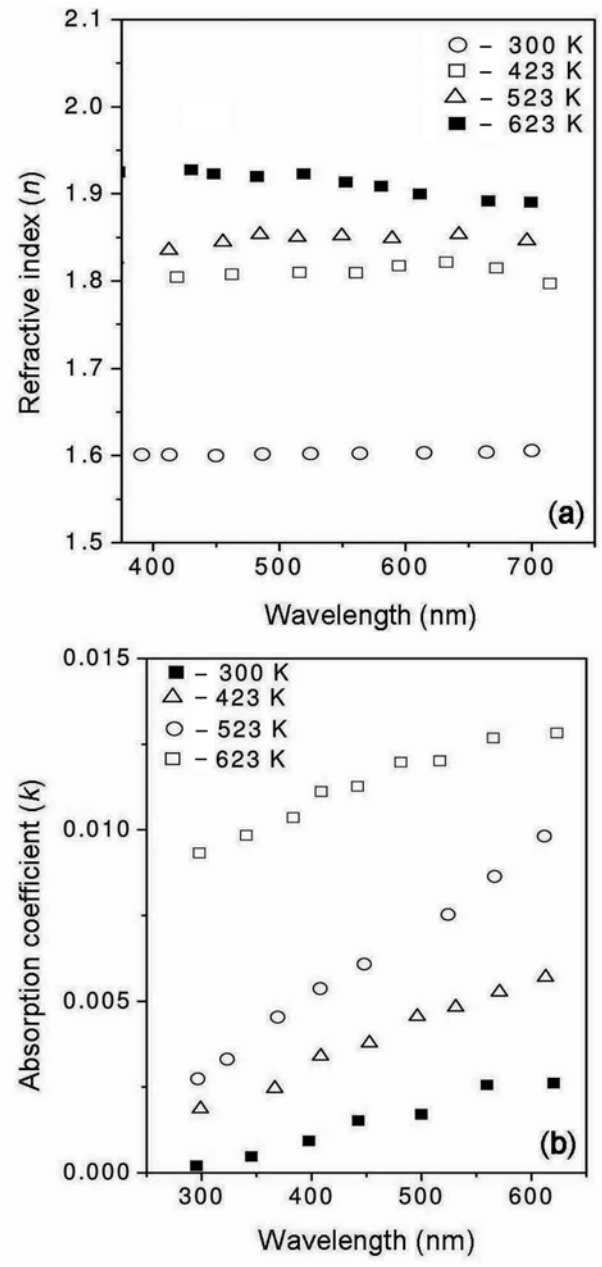

Figure 6. Variation of (**a**) refractive index (n) and (**b**) extinction coefficient (k) with energy for four representative Si-doped GaN films.

surface[21] considering a Gaussian distribution of the crystallite size (D)

$$P(D) = (D - D_{min})\,(D_{max} - D)\exp(-D^2/\delta^2), \quad (3)$$

where D_{max} and D_{min} are the maximum and minimum diameters of the grains and δ the half-width of the grain distribution; $D_{max} = \bar{D} + \delta$ and $D_{min} = \bar{D} - \delta$, $\bar{D}$ being the average radius. The distribution of grains thus obtained for films deposited at two different temperatures (corresponding SEM micrographs are shown in figure 1) is also shown in figure 1. Variation of the average grain

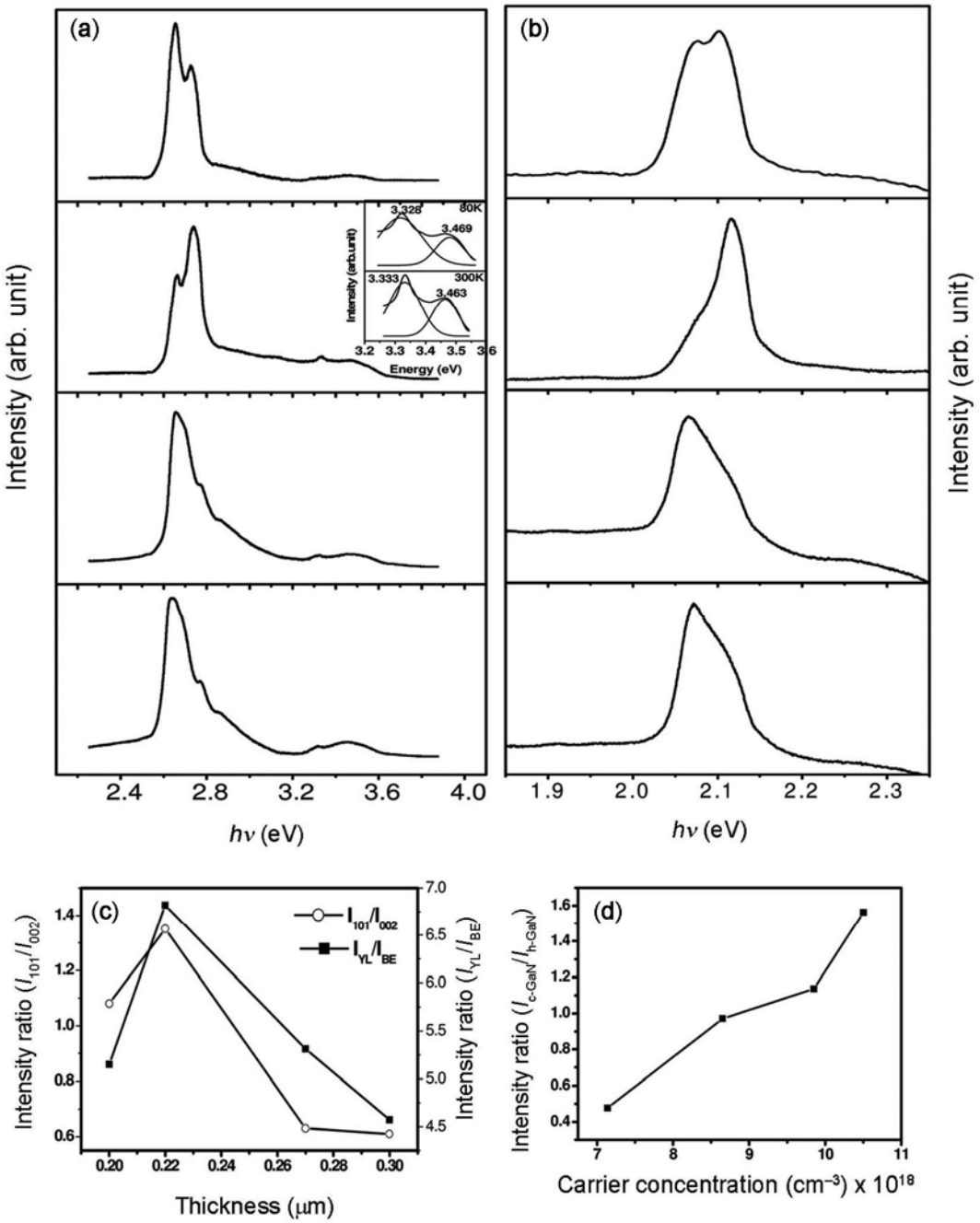

Figure 7. PL spectra of two representative Si-doped GaN films deposited (**a**) in the range of 320–550 nm and (**b**) in the range of 550–675 nm. (**c**) Intensity ratio of h-GaN to c-GaN and YL to BE emission with respect to grain size and (**d**) Intensity of $I_{\text{h-GaN}}/I_{\text{c-GaN}}$ with respect to carrier concentration.

diameter of our GaN films (thickness ~ 1 μm) deposited at different substrate temperatures has been shown in figure 5. This agreed well with that obtained from SEM studies.

3.4 *Photoluminescence (PL) studies*

PL measurements were recorded at 80 and 300 K by using a 300 W xenon arc lamp as the emission source. A Hamamatsu photomultiplier along with a 1/4 m monochromator was used as the detector. The spectra were recorded with excitation at 300 nm radiation for detecting PL peaks in the range 320–550 nm while for detecting peaks in the range 550–675 nm, an excitation energy of 435 nm was used. PL spectra were recorded as above at 80 K in the range of 320–550 and 550–675 nm as shown in figures 7a and b, respectively. The spectra were recorded at increasing substrate temperature

(300–623) from bottom to top. The luminescence at ~2.7 eV indicated blue emission (BE)[9] and could be identified as arising from the transitions between deep donor and induced shallow acceptor by Si impurity without *d* electron. The origin of the deep donor might be due to nitrogen vacancy[10] or Ga interstitial-related defects. There are two other peaks located at ~2.8 and ~2.85 eV (in the low-temperature region), which may result from radiative recombination related to the Urbach tail region and it was considered that it has a large potential fluctuation due to the grain to grain band discontinuity or the piezoelectric field, especially because of the coexistence of the grains with different orientations.[10,22] The transitions located between ~2.1 and 2.065 eV may be ascribed to the transitions between shallow donor and deep acceptor levels. This is the typical signature of yellow luminescence (YL) in GaN having multicomponent nature, which is very sensitive to the exact nature of distribution of the defects.[23] The deep acceptor levels might arise either due to Ga vacancy (V_{Ga}) or Ga vacancy with oxygen on a nitrogen site complex (V_{Ga}–O_N) and are the key defects responsible for YL in GaN.[6] The film surface is N rich in the presence of N_2 plasma and Ga rich in the presence of Ar plasma. Under N-rich condition the O_N (O on N sites) is less likely to form, which suppresses the formation of O_N–V_{Ga} complex. That is why it is preferred to continue the whole experiment using Ar plasma. Small PL peaks were located at high energy sides, ~3.46[4] and ~3.3 eV,[24] and could be identified as due to excitons bound to a neutral donor for h-GaN and c-GaN, respectively. Inset of figure 7a shows the room-temperature (300 K) and low-temperature (80 K) PL of a representative film in the BE emission region, which indicates the change in position, height and FWHM due to temperature difference. This is in conformity with the XRD and optical studies, which have indicated that the films contained both the h-GaN and c-GaN phases.

In order to determine the influence of structural defects on the YL emissions in the poly-GaN films both the intensity ratios of (101) to (002) diffraction peaks and YL and BE emissions are plotted in figure 7c, respectively. In general the intensity ratio of this diffraction peak is used to evaluate the crystalline quality of GaN films,[25] and that of YL to BE indicates the optical properties,[26] respectively. Considering the same trends between both intensity ratios of (101) to (002) peak and YL to BE emission, it was considered that the (101) atomic facet was associated with the YL in poly-GaN films on silica substrates. It was typically known that the gallium vacancies and impurity complexes, which were trapped at the structural defects such as dislocations and grain boundaries, were responsible for the YL emission in GaN materials.[27,28] Recently, it has been reported that the YL emission has been attributed to the atomic facets of (1010) and (1011) in GaN materials.[25,29]

3.5 *Carrier concentration determination from C–V analysis*

The carrier concentration (*N*) obtained from *C–V* analysis using Ag/GaN/SnO_2 Schottky diode structure[30] at a frequency of 100 kHz varied from 9.54×10^{18} to 2.48×10^{19} cm^{-3} with increasing substrate temperature, whereas in undoped sample it was noticed that it changed from ~10^{16} to 10^{17} cm^{-3}. To characterize the effect of Si doping on the h-GaN to c-GaN phase transformation, the intensity ratio $I_{h\text{-}GaN}/I_{c\text{-}GaN}$ with respect to carrier concentration is considered in figure 7d. As the carrier concentration is increased with the change in temperature, the fraction of c-GaN increased. The latter finding may be co-related with the bandgap transformation from h-GaN to c-GaN as shown in figure 5. The mechanism of phase transformation in GaN is generally thought to be due to stacking particle always in dislocations associated with it. The particle then grows by Si diffusion to its surface. The large volume change also requires that the Ga/N ratio of atoms should be displaced from the vicinity/matrix interface. This may be accomplished by the generation of interstitial Ga/N at the particle/matrix interface. This excess interstitials can form stacking faults.[31,32] These stacking faults in turn form the channels of the phase transformation.

4. Conclusion

Polycrystalline Si-doped GaN films were deposited with different grain sizes by varying the substrate temperature during r.f. sputtering of the GaN target. Grain size increased from ~0.2 to ~0.35 μm as the substrate temperature during deposition was increased from 300 to 623 K, which is in good agreement with optical measurements and XRD studies. The films showed predominant hexagonal structure when deposited at $T < 423$ K, while those deposited at $T > 523$ K were found to be rich in cubic phase. The XRD traces contained the signature of both the hexagonal and cubic phases of GaN. The PL peak at ~2.7 eV could be identified as arising due to the transitions between deep donor and induced shallow acceptor due to Si impurity without *d* electron. The (101) atomic facet was associated with the YL in poly-GaN films on silica substrates located between ~2.1 and 2.065 eV. Small PL peaks located at high energy sides, ~3.46 and 3.3 eV, could be identified as due to excitons bound to a neutral donor for h-GaN and c-GaN, respectively. Particle grows by Si diffusion through the film surface, and the variation of substrate temperatures are the reason of different proportions in cubic and hexagonal phases of the films. The carrier concentration varied from 9.54×10^{18} to 2.48×10^{19} cm^{-3} with increase in substrate temperature, whereas in undoped sample we have noticed that it changed from ~10^{16} to 10^{17} cm^{-3}.

References

1. Jenkins D W and Dow J D 1989 *Phys. Rev. B* **39** 3317
2. Neugebaur J and Van der Walle C G 1994 *Phys. Rev. B* **50** 8067
3. Li Z Q, Chen H, Liu H F, Wan L, Huang Q and Zhou J M 2001 *J. Cryst. Growth* **227–228** 420
4. Hasegawa S, Nishida S, Yamashita T and Asahi H 2005 *Thin Solid Films* **487** 260
5. Tampo H, Asahi H , Imanishi Y, Hiroki M, Ohnishi K, Yamada K, Asami K and Gonda S 2001 *J. Cryst. Growth* **227–228** 442
6. Yu H B, Chen H, Li D, Han Y J, Zheng X H, Huang Q and Zhou J M 2004 *J. Cryst. Growth* **263** 94
7. Park S E, Kim D J and Byungsung O 2003 *J. Cryst. Growth* **252** 87
8. Park S E, Kim D J, Woo S W, Lim S M and Byungsung O 2002 *J. Cryst. Growth* **242** 383
9. Maa H L, Yang Y G, Maa J and Liuc X M 2004 *Diam. Relat. Mater.* **13** 1892
10. Yang Y, Yu K and Zhang Y 2004 *Physica B* **352** 1
11. Maruyama T and Miyake H 2006 *J. Vac. Sci. Technol. A* **24** 1096
12. Chowdhury M P, Roy R K, Chakraborty B R and Pal A K 2005 *Thin Solid Films* **491** 29
13. Chen R, Zhou W and Kwok H S 2012 *Appl. Phys. Lett.* **100** 253501
14. Zou C W, Wang H J, Yin M L, Li M, Liu C S, Guo L P, Fu D J and Kang T W 2009 *J. Cryst. Growth* **311** 223
15. Niehus M *et al* 2004 *J. Non-Cryst Solids* **338–340** 460
16. Wang F Y, Wang R Z, Zhao W, Song X M, Wang B and Yan H 2009 *Sci. China Series F: Inform. Sci.* **52** 1947
17. Hong J-II, Chang Y, Ding Y, Wang Z L and Snyder R L 2011 *Thin Solids Films* **519** 3608
18. Lopez N P, Tao J H, McKittrick J, Talbot J B, Raukas M, Laski J, Mishra K C and Hirata G 2008 *Phys. State Sol. (C): Curr. Topics Solid State Phys.* **5** 1756
19. Bhattacharyya D, Chaudhuri S and Pal A K 1992 *Vacuum* **43** 313
20. Manifacier J C, Muricia M D, Fillard J P and Vicario E 1977 *Thin Solid Films* **41** 127
21. Bhattacharyya D, Chaudhuri S and Pal A K 1993 *Vacuum* **44** 797
22. Hiroki M, Asahi H, Tampo H, Asami K and Gonda S 2000 *J. Cryst. Growth* **209** 387
23. Kucheyev S O, Toth M, Phillips M R, Williams J S, Jagadish C and Li G 2002 *Appl. Phys. Lett.* **91** 5867
24. Rieger W, Dimitrov R, Brunner D, Rohrer E, Ambacher O and Stutzmann M 1996 *Phys. Rev. B* **54** 17596
25. Yang S H, Ahn S H, Jeong M S, Nahm K S, Suh E K and Lim K Y 2000 *Solid State Electron.* **44** 1655
26. Li X and Coleman J J 1997 *Appl. Phys. Lett.* **70** 27
27. Hansen P J, Strausser Y E, Erickson A N, Tarsa E J, Kozodoy P, Brazel E G, Ibbetson J P, Mishra U, Narayanamurti V, DenBaars S P and Speck J S 1998 *Appl. Phys. Lett.* **72** 2247
28. Timmers H, Chen A, Patrick P T, Weijers T D M, Goldys E M, Tansley T L, Elliman R G and Freitas J A 2002 *J. Appl. Phys.* **92** 3397
29. Li X, Bohn P W and Coleman J J 1999 *Appl. Phys. Lett.* **75** 4049
30. Deb B, Ganguly A, Chaudhuri S, Chakraborti B R and Pal A K 2002 *Mater. Chem. Phys.* **74** 282
31. Patel J R, Jackson K A and Reiss H J 1977 *J. Appl. Phys.* **48** 5279
32. Xu D, Yang H, Li J B, Li S F, Wang Y T, Zhao D G and Wu R H 1999 *J. Cryst. Growth* **206** 150